Přírodovědecká fakulta
Faculty of Science

Jihočeská univerzita v Českých Budějovicích
University of South Bohemia in České Budějovice

Bachelor thesis

The role of mitochondrial SCoAS substrate-level phosphorylation in the bloodstream form *T. brucei*

Michaela Husová

2019

Supervisor: RNDr. Alena Panicucci Zíková, PhD

Co-supervisor: Brian Panicucci

Husová, M., 2019: The role of mitochondrial SCoAS substrate-level phosphorylation in the bloodstream form *T. brucei*. Bc. Thesis, in English – 46 p., Faculty of Science, University of South Bohemia, České Budějovice, Czech Republic

Annotation:

Mitochondrial metabolism of Trypanosoma brucei is considered highly reduced because of its dysfunctional electron transport chain and tricarboxylic acid cycle. But previously published paper suggests significant mitochondrial ATP pool created by substrate phosphorylation via succinyl coenzyme A synthetase, which plays crucial role in *T. brucei* survival. This thesis is therefore focused on substrate phosphorylation and on influence of succinyl coenzyme A synthetase heterodimer RNAi on T. brucei cells.

I hereby declare that I have worked on my bachelor's thesis independently and used only the sources listed in the bibliography.

I hereby declare that, in accordance with Article 47b of Act No. 111/1998 in the valid wording, I agree with the publication of my bachelor thesis, in full form to be kept in the Faculty of Science archive, in electronic form in publicly accessible part of the STAG database operated by the University of South Bohemia in České Budějovice accessible through its web pages.

Further, I agree to the electronic publication of the comments of my supervisor and thesis opponents and the record of the proceedings and results of the thesis defense in accordance with aforementioned Act No. 111/1998. I also agree to the comparison of the text of my thesis with the Theses.cz thesis database operated by the National Registry of University Theses and a plagiarism detection system.

České Budějovice …….. ……

Michaela Husová

Acknowledgment:

I would like to thank Alena for this great opportunity to become part of the lab. I'd like to give special thanks to Brian for showing me everything, for helping me improve my skills and also for his patience and support. And I cannot forget about other members of the lab, thank you for your help and the for the nice and positive working environment.

Abbreviations:

10-CHO-THF	10-Formyl-Tetrahydropholate
AAC	ADP/ATP carrier
ASCT	acetate-succinate CoA-transferase
ACH	acetyl-CoA thioesterase
AOX	alternative oxidase
APRT	adenine phosphoribosyltransferase
ATP/ADP	adenosine triphosphate / diphosphate
BF	bloodstream form
BSA	bovine serum albumin
cDNA	complementary DNA
CoA	coenzym A
Ct	cycle threshold
DHCH	methylene-tetrahydrofolate dehydrogenase/cyclohydrolase
Dk	dyskinetoplastic cells
ETC	electron transport chain
FBS	fetal bovine serum
FTL	formyl-tetrahydrofolate ligase
GTP	guanosin triphosphate
HPLC	high performance liquid chromatography
HRP	horseradish peroxidase
mtHSP70	mitochondrial heat shock protein 70
OXPHOS	oxidative phosphorylation
PAb	polyclonal antibody

PBS	phosphate buffered saline
PBS-T	phosphate buffered saline with Tween20
PEPCK	phosphoenolpyruvate carboxykinase
PF	procyclic form
PVDF	polyvinylidene difluoride
qPCR	quantitative polymerase chain reaction
RT	reverse transcriptase
SCoAS	succinyl coenzyme A synthetase
SUBPHOS	substrate-level phosphorylation
SDS	sodium dodecyl sulfate
TCA	tricarboxylic acid cycle
VSG	variant surface glycoprotein
WCL	whole cell lysate

Table of contents:

1. Introduction 1

1.1. Trypanosoma brucei 1

1.2. *T. brucei* life cycle 1

1.3. *T. brucei* metabolism 2

1.3.1. Substrate phosphorylation 4

2. Aims of the Thesis 7

3. Materials and Methods 8

3.1. Cell cultures 8

3.1.1. Growing the cells 8

3.1.2. Cell counting 9

3.1.3. Liquid nitrogen stabilates 10

3.2. Growth curves 10

3.3. qPCR 11

3.3.1. Harvesting RNA 12

3.3.2. DNase Treatment 12

3.3.3. Reverse Transcription 13

3.3.4. qPCR sample preparation 13

3.3.5 qPCR calculations 13

3.4. Protein purification 14

3.4.1 Bacterial expression of SCoAS beta 14

3.4.2. Sarkosyl solubilization of recombinant SCoAS beta 15

3.4.3. High-performance liquid chromatography 17

3.4.4. Purification analysis by Coomassie staining 18

3.4.5. Dialysis 19

3.4.6. Protein concentration determination 20

3.5. Western blots 20

4. Results 22
4.1. SCoAS alpha RNAi growth curve 22
4.2. qPCR verification of RNAi induction 23
4.3. SCoAS beta antigen preparation 24
4.3.1. SCoAS beta protein purification profile 24
4.3.2. SDS PAGE 25
4.4. Testing SCoAS beta PAb 27
4.5. Verification of SCoAS cell lines 29
4.5.1. SCoAS beta RNAi 29
4.5.2. SCoAS alpha RNAi 30
4.5.3. MiTaT SCoAS beta RNAi 31
5. Discussion 32
6. References 36

1. Introduction

1.1. Trypanosoma brucei

Trypanosoma brucei is an extracellular parasite belonging to the class of Kinetoplastea, which is comprised of organisms with concatenated mini- and maxicircle mitochondrial DNA that forms a unique structure called the kinetoplast. *T. brucei* is a flagellated protist, with the flagellum attached to the cell membrane creating an undulating membrane. It is the causative agent of African trypanosomiasis, also known as sleeping sickness in humans and nagana in livestock. Sleeping sickness is transmitted by the tsetse fly and it is a threat to millions of people in 36 Sub-Saharan African countries. Most of the infected patients are from the Democratic Republic of Congo, where almost 1000 new cases are reported annually (www.who.int). There are two major subspecies of *T. brucei* that are largely restricted to different parts of Africa. *T. brucei gambiense* is a subtype found in Central and West Africa. Most cases of sleeping sickness is caused by this type. Infected patients are without clear symptoms of the disease for a long period of time. When the major symptoms emerge the disease is already in an advanced stage and the nervous system of the host is already under attack. While lethal if untreated, undiagnosed patients can survive an average of 3 years without therapeutics. On the other hand, *T. brucei rhodesiense* causes a more acute form of the disease. It occurs more in the East and Southeast regions of Africa, but it is only responsible for about 3% of all sleeping sickness cases. Symptoms emerge within weeks as the human pathogen rapidly invades the host's nervous system, leading to mental deterioration and death (www.cdc.gov). Drugs currently used aren't sufficient, there is increasing drug resistance, and they have severe side effects (*Croft et al,* 2005). It also creates economic problems when domesticated animals become infected, which is a huge burden for people in rural Africa.

1.2. *T. brucei* life cycle

Trypanosoma brucei has complex life cycle that alternates between a mammalian host and the tsetse fly. The parasite is pleomorphic, meaning that the cell morphology changes as they differentiate between multiple cell types. Briefly, the procyclic form (PF) in the insect vector immediately adapts to the mammalian blood and transitions into a proliferative bloodstream form (BF). In order to prevent the rapid death of the host, these long slender BF parasites differentiate into a nonproliferating stumpy form (*Mony et al,* 2015). These are pre-adapted to survive in tsetse fly and they can survive the temperature and pH differences between the host bloodstream and the tsetse fly midgut (Rico *et al,*

2013). Production of these stumpy forms is a form of quorum sensing that maintains a balance between stumpy and slender forms to increase the chance for transmission by the insect vector to a new host (Rico *et al,* 2013). Stumpy forms are destined for transmission or death (Fenn *et al,* 2007). When they are taken up by the tsetse fly, they undergo morphological and metabolic changes as they differentiate into the procyclic forms (Rico *et al,* 2013). Full parasite development within the fly takes between 20-30 days, during which the parasite undergoes many changes to become capable of infecting a mammalian host (Fenn *et al,* 2007). The late metacyclic forms found in the salivary glands are transmitted to the mammal host during a blood meal.

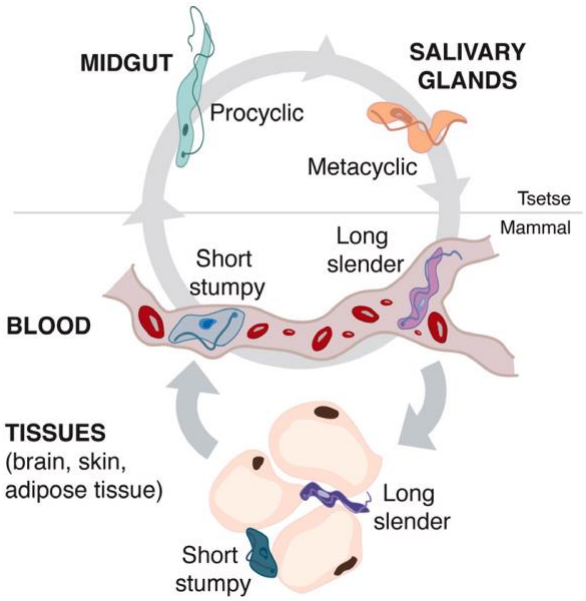

Figure 1. Life cycle of *Trypanosoma brucei*. The parasites undergo several main changes during their life cycle. In the mammalian host, long slender forms differentiate into stumpy forms, which are adapted to survive in the insect vector. Procyclic cells in the insect midgut undergo metabolic and morphological changes as they traverse to salivary glands and differentiate into metacyclic cells that are capable of infecting a new host. (*Smith et al,* 2017)

One of the most important adaptations during the life cycle is antigenic variation. BF *T. brucei* has a surface coat made of a variant surface glycoprotein (VSG) that protects it from lytic factors in the host blood (*Burri et al,* 2014). The VSG protein coat can be changed often to stay ahead of the host's immune system (Fenn *et al,* 2007) (Berrimann *et al,* 2005).

1.3. *T. brucei* metabolism

As the parasite completes a life cycle, it must rapidly adapt its metabolism to the very different environments it inhabits. While BF *T. brucei* utilize the abundant glucose found in the bloodstream of the host, PF parasites in the insect midgut must rely on the amino acids proline and threonine for their main carbon sources. These varied environments also cause significant changes to the ultrastructure of the single mitochondrion of BF and PF

parasites. While the PF mitochondrion is highly branched with discoidal cristae, the BF organelle has a narrow tubular mitochondrion without cristae (*Smith et al,* 2017).

PF *T. brucei* create their ATP pool mainly by oxidative phosphorylation (OXPHOS). OXPHOS is a process that oxidizes reduced cofactors produced by the catabolism of various carbon sources to create ATP. Electrons from the reduced cofactors are transferred through the electron transport chain (ETC) and their energy is used to pump protons into the intermembrane space. This potential energy of proton gradient is converted into mechanical energy as the protons are allowed to flow down their gradient and enter the mitochondrial matrix by passing through the proton pore of the F_OF_1-ATP synthase. This causes the ATP synthase to rotate and create chemical energy in the form of ATP. In a glucose-poor environment, PF parasites mainly catabolize proline in the mitochondrion (*van Hellemond et al,* 2005), creating several reduced cofactors that are used for ATP production in OXPHOS. But their tricarboxylic acid (TCA) cycle is not completely formed, as not all of the acetyl-CoA created from proline is oxidized and part of it is converted into acetate and used in the biosynthesis of lipids. Interestingly, when the PF cells are cultivated in the glucose rich medium, they prefer glycolysis even in the presence of proline (*Bringaud et al,* 2006), showing how flexible the *T. brucei* cells are. Glucose is catabolized into pyruvate, which is further converted into the excreted end products of succinate or acetate, the latter generated by acetate-succinate CoA-transferase (ASCT) (*Smith et al,* 2017). During these reactions, ATP is created by substrate-level phosphorylation (SUBPHOS). ATP produced in the mitochondrion is then transported by the ADP/ATP carrier (AAC) into the cytoplasm.

The energy metabolism of the BF *T. brucei* is very different. Since the host bloodstream contains high levels of glucose, it appears that intensive glycolysis is sufficient for all ATP requirements. Since the pyruvate created by glycolysis is mostly excreted out of the cell, it is not further oxidized by fermentation to generate lactate. Therefore, the reduction-oxidation (redox) balance is maintained by the oxidation of glycerol-3-phosphate by the glycerol-3-phosphate dehydrogenase, with the electrons being passed on to the alternative oxidase (AOX) (*Zíková et al,* 2017). Furthermore, BF parasites lack the cytochromes required for a functioning ETC. Without these proton-pumping enzymes to generate a proton gradient, the F_oF_1-ATP synthase reverses it rotation and begins to hydrolyze ATP. This energy is then used by the ATPase to pump protons into the mitochondrial intermembrane space to maintain the mitochondrial membrane

potential, which is essential for the import of mitochondrial proteins (*Schnaufer*, et al. 2005). It is generally accepted that the mitochondrial ATP consumed in this process is imported from the cytosol by AAC. This assumption was made because it was long thought that the TCA cycle did not function in the BF mitochondrion. However, a comparison of the BF and PF mitoproteome showed a surprisingly 80% similarity. Essential TCA enzymes were found in the BF cells, albeit with lower expression levels than the PF parasites (*Zíková et al*, 2017). These data suggest that there might also be SUBPHOS occurring in the mitochondrion, not only in the cytoplasm via glycolysis. This hypothesis is supported by the data published by Zhang et al, where the RNAi of succinyl-CoA synthetase (SCoAS) beta produced a strong growth phenotype.

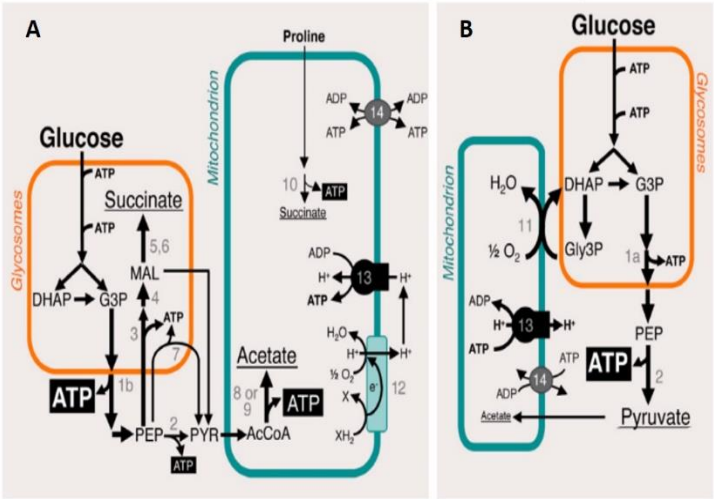

Figure 2: Main metabolic pathways in (A) procyclic forms and (B) in bloodforms. PF cells have a unique TCA cycle, creating ATP and reduced cofactors. In BF parasites, ATP derived from glycolysis is imported by AAC into the mitochondrion, where it is consumed by ATPase to maintain the mitochondrial membrane potential. (*Smith et al,* 2017)

1.3.1. Substrate phosphorylation

In this thesis, we would like to explore what is the source of BF mitochondrial ATP that must be consumed by the ATPase to maintain the mitochondrial membrane potential. While it is widely believed that the TCA cycle is not active during this life cycle stage, there is an increasing amount of evidence suggesting that maybe the few TCA enzymes required for SUBPHOS are present. While OXPHOS utilizes the proton motive force generated by the ETC to generate ATP, SUBPHOS couples the energy released from catabolic reactions to add a terminal inorganic phosphate to ADP. SUBPHOS mostly occurs during glycolysis and the TCA cycle. The transfer of phosphate between molecules is catalyzed by enzymes called kinases, such as phosphoenolpyruvate carboxykinase (PEPCK) or SCoAS. PEPCK is one of the most important enzymes creating ATP by

substrate phosphorylation during glycolysis. In *T. brucei*, glycolysis occurs in glycosomes, which are specialized organelles that resemble peroxisomes (*Sommer* et al, 1994). The activity of PEPCK is dependent on the ATP levels in the cell (Formula 1) (*Hunt* et al, *1995*). Since PEPCK is localized to the glycosome, which does not possess a carrier to transport ATP, the ATP produced by this enzyme cannot be the source of mitochondrial ATP.

$$\text{ATP} + \text{oxaloacetate} \rightleftharpoons \text{ADP} + \text{Phosphoenolpyruvate} + CO_2$$

Formula 1: Reaction catabolized by PEPCK

Another common SUBPHOS enzyme is formyl-tetrahydrofolate ligase (FTL). This enzyme is involved in catabolic reactions that produce 10-Formyl-Tetrahydropholate (10-CHO-THF) (Formula 2). 10-CHO-THF is used for the *de novo* synthesis of purines, an anabolic pathway missing within Trypanosomatida. Therefore, *T. brucei* mainly utilizes 10-CHO-THF for the formylation of the mitochondrial methionyl-tRNA, an essential process required for mitochondrial translation. FTL was found in all Trypanosomatida except for *T. brucei*. (*Eadsforth* et al, 2012). There is another bifunctional enzyme, called methylene-tetrahydrofolate dehydrogenase/cyclohydrolase (DHCH), that is capable of producing 10-CHO-THF (Formula 3). While DHCH was previously identified in *T. brucei*, it is localized in the cytoplasm and has no direct contribution to the mitochondrial ATP pool (*Vickers* et al, 2009).

$$\text{ATP} + \text{formate} + \text{tetrahydrofolate} \rightleftharpoons \text{ADP} + \text{phosphate} + \text{10-CHO-THF}$$

Formula 2: Reaction catabolized by FTL.

$$\text{5,10-methylenetetrahydrofolate} \rightleftharpoons \text{5,10-methenyltetrahydrofolate.}$$

$$\text{5,10-methenyltetrahydrofolate} \rightleftharpoons \text{10-CHO-THF}$$

Formula 3: Reactions catabolized by DHCH. The first reaction is catabolized by the dehydrogenase and the second by a cyclohydrolase.

The last known enzyme involved in SUBPHOS is SCoAS. SCoAS catalyzes the reaction of succinyl-coenzyme A to succinate, while creating coenzyme A (CoA) and ATP or GTP (Formula 4). The enzyme is a heterodimer, composed of an alpha and beta subunit. The beta subunit has two isoforms that are around 53% similar to each other (*Johnson et*

al, 1998). Therefore, the specificity of SCoAS for either GTP or ATP is determined by which beta isoform is present. It was published that *T. brucei* SCoAS prefers to synthesize ATP compared to GTP (*Jenkins et al,* 1988). Interestingly, both nucleotides can be used as phosphate donors in the reverse reaction. SCoAS activity is regulated by the intracellular ATP concentration (*Hunger-Glasser et al,* 1999).

$$NDP + Pi + Succinyl\text{-}CoA \rightleftharpoons NTP + Succinate + CoA$$

Formula 4: Reaction catabolized by SCoAS.

ATP can be produced by two independent pathways that include SCoAS. One converts alpha-ketoglutarate to succinate. In PF *T. brucei*, the catabolism of glutamine creates alpha-ketoglutarate, which is then converted to succinyl-CoA. SCoAS then produces ATP as it catalyzes succinyl-CoA into succinate. It was presumed that SCoAS has no crucial role in the BF stage because of their simplified mitochondrial metabolism, but the genetic evidence provided by Zhang et al, suggests otherwise. They reported a rapid growth phenotype was observed after 20 hours of SCoAS beta RNAi.

The other SUBPHOS pathway converts threonine or pyruvate into acetate through acetyl-CoA, which produces ATP (*van Hellemond et al,* 1998). For PF cells, threonine catabolism is important for lipid synthesis. The pyruvate used in this pathway is derived from glycolysis or alanine metabolism (*Bringaud et al,* 2006). It was also shown in unpublished data from our lab that BF parasites can uptake threonine (*Taleva,* 2016). Acetyl-CoA created in this way is then converted in the mitochondrion to acetate. This process can be catalyzed by either acetyl-CoA thioesterase (ACH) or by ASCT (*Millerioux et al,* 2012). ACH does not create any ATP during this process, but ASCT activity is coupled to SCoAS and creates a significant amount of ATP (*Taleva,* 2016). Complicating matters, these two redundant, parallel pathways can complement the function of each other and produce the essential acetate from acetyl-CoA.

2. Aims of the Thesis

The aims of this thesis include the following:

- Determining if SCoAS alpha is essential in BF *T. brucei*
- Evaluating SCoAS alpha RNAi efficiency by qPCR
- Preparation of SCoAS beta antigen for antibody production
- Analyzing the SCoAS beta polyclonal antibody
- Verification of SCoAS RNAi depletion by western blot analysis

3. Materials and Methods

3.1. Cell cultures

The most common lab strain studied is BF *Trypanosoma brucei* Lister 427. This cell line was originally isolated in 1960 from a sheep in Uganda before Keith Vickerman transferred it in 1961 to the Lister Institute in London (Cross, 1973). Since BF *T. brucei* are able to routinely exchange the uniformly expressed variable surface glycoprotein (VSG) on their cell surface, different clones of the parasite were originally defined by the VSG being expressed. The location where the antigen type was originally defined lends itself to the name, e.g., Molteno Institute trypanozoon antigen type. In this thesis, we analyzed BF *T. brucei* Lister 427 MiTat 1.2 (a generous gift from the Bringaud lab) and a Lister 427 with an unknown MiTat antigenic type (Zíková lab strain). Most likely, this cell line is also a Lister 427 MiTat 1.2, but that has not been verified. Throughout the rest of the thesis, we will refer to the Zíková lab strain simply as BF *T. brucei* Lister 427, while the other defined cell line will be referenced specifically as BF *T. brucei* Lister 427 MiTat 1.2. Since we want to perform regulatable RNAi in these cell types, we are using genetically modified cell lines that contain the T7 RNA polymerase and the bacterial Tet repressor. The heterologous expression of these two proteins in the BF *T. brucei* Lister 427 MiTat 1.2 cell line is the result of transfecting two different expression vectors and is now referred to as 90-13 after the designation of the vectors (Wirtz, 1999). In comparison, the BF *T. brucei* Lister 427 cell line was tranfected with just a single vector that contained both heterologous proteins as is referred to as BF *T. brucei* Lister 427 single marker (SM) (Poon, 2012).

3.1.1. Growing the cells

Cultures of BF *T. brucei* were grown in HMI-11 media (Table 1) and usually maintained in 5 ml of media in 25cm^2 flasks. When bigger numbers of cells were needed for an experiment, 100-150 ml cultures were grown in 150cm^2 flasks. Cells need to be grown at 37°C and with 5% CO_2, which interacts with the bicarbonate in the media to maintain a physiological pH. Therefore, the lids of the tissue culture flasks were left slightly loose. Phenol red was also included in the media as a pH indicator, as it turns orange under acidic conditions. BF T. brucei cells grow rapidly with a doubling time of about 6 hours. Generally, it is important to maintain BF cells within mid-log phase growth by regularly splitting them before they reach stationary phase around 2-3x10^6 cells/ml. While BF cultures cannot grow too dense, they are just fine when split harshly. Therefore,

to maintain a healthy culture, we remove all but the last few drops of a culture and add fresh media every two days. When a dense culture is required for the following day, they can be split 1:10 or to $2x10^5$ cells/ml. Cultures were routinely checked under an inverted light microscope to observe the motility and morphology of the cells. Healthy BF cells move rapidly in a tumbling manner, have an elongated shape and are actively dividing. Cells that are stressed move less and have either a very long skinny morphology or a very rounded shape.

Table 1: HMI-11 + 10% FBS media

Reagent	Quantity per 10L of media
Invitrogen HMI-11 premix	181,4g
Sodium bicarbonate	30g
Penicilin/Streptomycin	100ml
The final volume adjusted with MilliQ water to	9,0L
FBS	1L

3.1.2. Cell counting

Since experiments often required a set number of cells, the cell culture density was measured with a Z2 Coulter Counter (Beckman Coulter Inc.). It consists of a probe with two electrodes that is immersed into the cells suspended in a conductive diluent. This creates an electric current between the electrodes. Non-conductive cells cause a decrease in the current when passing through the channel between the electrodes. This change of voltage is equal to the cell volume passing through the channel. Determining the density of cells in a small volume allows us to extrapolate and calculate the density of the whole culture. Counting cells involved mixing 100µl of culture with 100µl of the Trypanosomatid Cell Fix Solution (Table 2), which render the parasites noninfectious. 50µl of the fixed cells was then added to 5ml of Hemasol in a 10ml cuvette. The cuvette with the cell sample was placed in the counter and the final cell density was calculated by the computer using the previously entered dilution factor.

Table 2: Trypanosomatid Cell Fix Solution

Reagent	Stock	Amount	Final
dH_2O		85ml	
SSC	20x	5ml	1x
Formaldehyde	36%	10ml	3,6%

3.1.3. Liquid nitrogen stabilates

After a new cell line was generated, stabilates were made for long-term storage. It was imperative that the cultures were healthy. They need to be dividing at a normal rate for several days and have good morphology and movement. When the cell density reached 1-2x10^6 cells/ml, stabilates were created in the tissue culture hood by mixing 500µl of the cell culture with 500µl of the Bloodform Freezing Solution (Table 3.) in a properly labeled cryovial. Cryovials were left on ice for 30 minutes and then placed in a -80°C freezer for 3 days. After this slow cooling phase, the stabilates were transferred into the liquid nitrogen tank. When the cells were needed again, the cryovials were taken out of the tank and left to thaw at room temperature. When completely thawed, 1ml of the solution was transferred into a 25cm^2 flask containing 9ml of HMI-11 media. The motility and morphology of the cells were monitored for the next few days to make sure they were not damaged by the freezing process.

Table 3: Bloodform Stabilate Freezing Solution

Reagent	FW or Stock	500ml	Final
MilliQ		200ml	
Glucose	180,16	9,3g	100mM
NaCl	58,44	2,1g	72mM
Sodium Citrate	294,1	0,75g	5mM
BSA	66,78	0,5g	15mM
Glycerol	80%	75ml	12%

3.2. Growth curves

To determine if the function of a gene product is essential for a cell, we measure the cell density of RNAi induced cell cultures every day for 7-10 days. A growth phenotype will manifest in the reduced doubling time of the RNAi induced culture compared to the uninduced culture. Several clones of each RNAi cell line were analyzed, with each clone split into two 25cm^2 flasks that would represent either the untreated or RNAi induced cultures. All cultures were measured and split to 1x10^5 cells/ml every day to maintain them in mid-log phase. All the following calculations were made in an Excel sheet to determine the cumulative density of a culture grown in a theoretical flask that is large enough to measure the growth curve without ever having to split the culture.

$$V\ left = \frac{cells\ needed}{cells\ counted}$$

Equation 1: Calculation of volume left in the flasks

$$V\ new\ = 5 - V\ left$$

Equation 2: Calculation of volume of new media to add

Volume left in the flask was used for calculating the dilution, which was further used for calculating the cumulative density after measuring the cell density on the next day.

$$\text{Dilution} = \frac{5}{V\ left}$$

Equation 3: Calculation of dilution

$$\text{Cumulative dilution} = \frac{dilution\ yesterday}{dilution}$$

Equation 4: Calculation of cumulative dilution

$$\text{Cumulative density} = \frac{density}{dilution\ yesterday}$$

Equation 5: Calculation of cumulative density

3.3. qPCR

Quantitative PCR (qPCR) is a method to quantify the amount of a specific transcript. RNA isolated from the cells is used to create a more stable template of complementary DNA (cDNA) using a reverse transcriptase enzyme. Then, similar to a regular PCR, this template is used in a DNA amplification reaction that includes cycles of the following three steps: denaturation, annealing and elongation. However, it is performed in a special cycler that can continuously detect the fluorescence of a fluorochrome, in this case SyberGreen, that can only emit light when it interacts with DNA. As the DNA accumulates in every cycle, the detected fluorescence signal becomes more intense. The resulting amplification plots are then used to define the cycle threshold (Ct) value for each gene. This value must be greater than the background fluorescence, but is otherwise arbitrarily selected to intersect the linear phase of the amplification plot of each gene. Combining the Ct value with the PCR efficiency of a set or primers, the absolute amount of a specific gene transcript can then be determined from a standard curve. Alternatively,

the relative amount of the target gene can be compared to an internal reference gene such as tubulin or 18S. These controls are chosen because they are highly transcribed and their population remains stable under all but the most severe stress conditions.

3.3.1. Harvesting RNA

Using the RNeasy Mini Kit (Qiagen), RNA was isolated from both noninduced cells and RNAi cultures induced for 2 and 4 days. $1x10^8$ cells of each clone were spun down at 1300g at room temperature for 10 minutes. The pellet was resuspended in 1ml of phosphate buffered saline (PBS) containing 13mM glucose and spun down the same way again. Any trace of liquid was discarded by an aspirator. The cell pellet was thoroughly resuspended in 600µl of RLT buffer before 600µl of ethanol was added. After the sample was mixed by pippeting, it was transferred to an RNeasy spin column and centrifuged for 15 seconds at 8000g. The column was first washed with 700µl of RW1 buffer and then with 500µl of RPE buffer. To elute the RNA, 50µl of RNase free water was added to the column and centrifuged for 1 minute at 8000g. The concentration of all RNA samples was measured on the Nanodrop spectrophotometer (Thermo Scientific).

3.3.2. DNase Treatment

Any contaminating traces of DNA in the RNA samples need to be degraded before the reverse transcription and qPCR steps. TURBO DNase (Ambion) is endonuclease that hydrolyzes double stranded DNA molecules in the presence of Mg^{2+} and Ca^{2+} ions. 10µg of RNA from each clone was treated with 1µl of TURBO DNase in a 50µl total volume reaction and incubated at 37°C for 30 minutes. After the DNase treatment, RNA samples were cleaned up with the RNeasy MinElute Cleanup kit (QIAGEN), where RNA is bound to a silica membrane in a spin column and any contaminants are washed away. Sample volumes were adjusted to 100µl and mixed with 350µl of RLT buffer. 250µl of 96% ethanol was added and the solution was loaded onto the spin column and centrifuged for 15 seconds at 11,000g. Spin columns were transferred into a new collection tube and washed with 500µl of RPE buffer. Then the RNA was washed with 500µl of 80% ethanol. The column was transferred to a new collection tube and spun down for 5 minutes at full speed to remove any traces of ethanol. The RNA was then eluted with RNase-free water. The concentration and purity of the RNA after the cleanup was again measured on the NanoDrop.

3.3.3. Reverse Transcription

The isolated RNA is then transcribed into cDNA by a reverse transcriptase (RT). 2µg of each RNA sample was mixed with DEPC water, 2µl of 10x RT buffer, 1,4µl of $MgCl_2$, 4µl of dNTP, 1µl of RNase inhibitor, 1µl of MultiScribe Reverse Transcriptase and 1µl of random hexamers. A second set of RNA samples were prepared without the RT to serve as negative control. All samples were then incubated in a thermo cycler for 10 minutes at 25°C, followed by 30 minutes at 37°C and finally for 5 minutes at 95°C.

3.3.4. qPCR sample preparation

For the purposes of this thesis, tubulin and 18S were used as a control genes for the comparison of SCoAS alpha transcription. First, forward and reverse primers for each gene were mixed together for a final concentration of 1,5uM. Then a qPCR master mix for all cDNA samples was made by mixing 65µl of MilliQ, 52µl of primer mix, 130µl of 2x SyberGreen. Reference genes were diluted 1:500. 10µl of the master mix was pipetted into 96 well plates containing 2µl of cDNA. The cDNA generated from each RNA sample was prepared in triplicate and included a negative control. The plate was then centrifuged at 400g for 3 minutes and inserted into the Roche Light Cycler 480. A program for the qPCR was set up and initiated.

3.3.5 qPCR calculations

Using a linear regression application, the PCR efficiency of each primer pair was calculated. These values were then entered into the LightCycler analysis program to calculate the Ct values. The Ct and PCR efficiency values were then used to calculate the ratio of the target transcript to the internal reference transcripts, according to the Pfaffl method (Pfaffl, 2001). The Pfaffl numerator was calculated from the target PCR efficiency and the Ct values for both the treated (RNAi induced) and untreated (noninduced) target transcript. Reference genes were used the same way to calculate the Pfaffl denominator.

$$Pfaffl\ numerator = \frac{Target\ efficiency}{Untreated - treated\ target}$$

Equation 6: Calculation of Pfaffl numerator.

$$Pfaffl\ denumerator = \frac{Control\ efficiency}{Untreated - treated\ control}$$

Equation 7: Calculation of Pfaffl denumerator.

$$Transcription\ ration = \frac{Pfaffl\ numerator}{Pfaffl\ denumerator}$$

Equation 8: Calculation of final transcription ratio of target and control gene.

3.4. Protein purification

There are numerous ways to purify a protein from a complex mixture. The best methods depend on the protein that is being isolated and how that protein will be used in downstream applications. One of the most common ways to produce a recombinant protein, is to utilize column chromatography for the affinity purification of a 6x histidine (His) tagged protein expressed in bacteria. This method was applied to purify the recombinant *T. brucei* SCoAS beta protein. Since the protein was previously determined to be secluded to the insoluble fraction of lysed bacteria, the purification scheme implemented sarkosyl to solubilize the recombinant protein.

3.4.1 Bacterial expression of SCoAS beta

Two 50ml overnight cultures of *E.coli* BL21 containing the pSKB3 expression plasmid for SCoAS beta were spun down at 500g for 10 minutes. Each cell pellet was resuspended in 5ml of LB broth (Table 4) and added to a previously prepared 2L erlenmeyer flask conatining 1L of autoclaved LB broth and 1ml of 50mg/ml kanamycin. The erlenmeyer flasks were incubated in a shaking incubator at 37°C. Once the optical density of the bacterial cultures exceeded 0,4, 1ml of 1M IPTG (Table 5) was added to induce protein expression. After 3 hours in a shaking incubator, the bacterial cultures were spun down at 4500g for 15 minutes. The cell pellet was then resuspended in 20ml of PBS and spun down again. After the supernatant was decanted, the pellets were flash frozen in liquid nitrogen and then stored at -80°C.

Table 4: LB media

Reagent	**FW**	**Amount**	**Final**
MilliQ		1600ml	
Tryptone		20,0g	
Yeast extract		10,0g	
NaCl	58,45	10,0g	171mM
pH~ 7.3 with NaOH			

Table 5: IPTG solution

Reagent	FW	Amount	Final
MilliQ		7ml	
IPTG	238,1	2,4g	1M
The final volume adjusted to (Qs):		10ml	

3.4.2. Sarkosyl solubilization of recombinant SCoAS beta

After a few days, one of the cell pellets was weighed to determine that it should be resuspended in 60ml of STE (Table 6) to achieve the recommended ratio of 30ml STE/g of bacteria. The STE buffer was prepared with a 2x concentration of the protease inhibitors included in the complete EDTA-free Protease Inhibitor Cocktail (Roche) tablets. The cell suspension was then split into three 50ml conical tubes and 20ml of STET buffer (Table 7) was added. Freshly prepared 10mg/ml lysozyme (Table 8) was added in a 1:10 dilution. After rotating for 40 minutes at 4°C, $MgCl_2$ was added in a 1:33 dilution. Finally, DNase I (Table 9) was added in a 1:2000 dilution and the solution was rotated for 10 minutes at 4°C. The tubes were then spun down at 10,000g for 30 minutes at 4°C. A sample of the supernatant was taken and mixed with 3xSDS PAGE loading dye to be used to analyze the purification later.

Table 6: STE Buffer

Reagent	Stock	Amount	Final
MilliQ		91,8ml	
Tris-HCl, pH 8.0	1M	5ml	50mM
NaCl	5M	3ml	150mM
EDTA	500mM	200µl	1mM

Table 7: STET Buffer

Reagent	Stock	Amount	Final
MilliQ		72,8ml	
Tris-HCl, pH 8.0	1M	5ml	50mM
NaCl	5M	3ml	150mM
EDTA	500mM	200µl	1mM
Triton X-100	10%	20ml	2%

Table 8: Lysozyme

Reagent	Stock	Amount	Final
MilliQ		4,5ml	
Tris-HCl, pH 8.0	1M	50µl	10mM
Lysozyme		50mg	10mg/ml

Table 9: DNase I

Reagent	Stock	Amount	Final
MilliQ		345µl	
Tris-HCl, pH 7.5	1M	10µl	10mM
NaCl	5M	10µl	50mM
$MgCl_2$	1M	10µl	10mM
DTT	1M	1µl	1mM
Glycerol	80%	625µl	1mM
DNase I		10mg	10mg/ml

To remove traces of the Tris buffer, all three individual pellets were pooled and resuspended in a total of 30ml PBS and spun down again. 2,25ml of 20% sarkosyl was added to the pellet for a final concentration of 1,5%. The tube was left rotating overnight at 4°C. The next day, the suspension was centrifuged at 10,000g for 30 minutes at 4°C to remove the insoluble material. A sample was taken from the supernatant, mixed with 3xSDS dye and saved to analyze the purification. The rest of the supernatant was transferred to a new tube. The insoluble pellet was resuspended in 30 ml PBS and a sample was again taken for later analysis. The supernatant was filtered through a syringe filter and an equal volume of Buffer A (Table 11) was added.

Table 10: Imidazol solution

Reagent	FW	Amount	Final
MilliQ		125ml	
Imidazole	68.08	42,55g	2,5M
HCl/NaOH		pH 6,0	
Qs		250ml	

Table 11: Buffer A solution

Reagent	Stock	Amount	Final
MilliQ		320ml	
$NaPO_4$	0,1M	100ml	20mM
NaCl	5M	50ml	500mM
Imidazole	2,5M	5ml	25mM
Sarkosyl	20%	25ml	1%

3.4.3. High-performance liquid chromatography

High-performance liquid chromatography (HPLC) can be used in different aspects to separate molecules based on their chemical properties. We employed affinity column chromatography to purify the recombinant His-tagged SCoAS beta protein over a Ni-NTA column. Once the protein was bound to the column, it was washed to remove any contaminants before being eluted by a gradient of imidazole that competes with the histidine residues to bind the nickel column.

In order to preserve the integrity of the Ni-NTA column, it is essential that all solutions are degassed to remove any air bubbles. Then we prepared the ÄKTAprime plus (GE) by flushing the tubes with ethanol to removing any air bubbles. With the bubbles removed, the Ni-NTA column was connected to the AKTA and washed with 20% ethanol for 10 minutes. Then the column was washed with MilliQ water for 15 minutes to remove any traces of ethanol. The next step was to prime the A and B tubes for chromatography. The B tubing was placed into a container of buffer B (Table 12) and the concentration was set to 100% with the inject valve position set to the waste position so buffer B with high imidazole concentrations does not enter the column. This process was followed by priming the A tubing and equilibrating the column. Tube A tube was placed in a container of buffer A and the concentration of buffer B buffer was set to 0% with the inject valve position to load. After 15 minutes of equilibration, the baseline for the UV sensor was established. Meanwhile the fraction collector with 60 glass tubes was aligned.

With the AKTA prepared, 60ml of the solubilized SCoAS beta sample was loaded onto the column through the A tubing. The flow rate was set to 1ml/min and the fraction size was set to 5ml. In order to avoid any bubbles being loaded onto the column, the last portion of the protein sample at the bottom of the graduated cylinder was left behind. Tube A was placed back into buffer A and the column was washed for several minutes. Once the UV trace that detects proteins exiting the column reached a new minimum, the

conditions for the elution of the SCoAS beta protein were established. The imidazole gradient was set to 50ml, with the inital concentration of buffer B set to 0% and the final to 100%. The flow rate was set to 1ml/min and the fraction size to 2ml. The UV trace was observed to detect which fractions contained a peak of our eluted protein.

Table 12: Buffer B solution

Reagent	Stock	Amount	Final
MilliQ		225ml	
$NaPO_4$	0,1M	100ml	20mM
NaCl	5M	50ml	500mM
Imidazole	2,5M	100ml	500mM
Sarkosyl	20%	25ml	1%

3.4.4. Purification analysis by Coomassie staining

To analyze the success of the purification, SDS-PAGE samples were prepared from the even numbered elution fractions along with the samples collected during the protein preparations process. 100µl of several flow through and elution fractions were taken, mixed with 50µl of 3xSDS PAGE loading dye and boiled at 97°C for 8 minutes. 4-20% precast polyacrylamide gels by BioRad were used to resolve the proteins. Meanwhile all fractions in the fraction collector were kept in 4°C. The SDS PAGE gels were stained with Coomassie Blue after the electrophoresis. Coomassie is a dye that binds to proteins through the sulfonic acid groups in the dye and the amine groups in the proteins. First, the protein gels were placed into plastic boxes filled and incubated on the orbital shaker for 5 minutes with distilled water to wash away any excess of SDS. After removing the water, the gels were covered with a fixing solution (Table 13) and again incubated on the shaker for 30 minutes. Next the gels were stained with the Coomassie dye (Table 14) and left on the shaker for 30 minutes. At last the gels were covered with a destain solution (Table 15) and left on the shaker overnight.

Table 13: Fixing Solution

Reagent	Amount	Final
dH_2O	200ml	
Methanol	250ml	50%
Acetic Acid	50ml	10%

Table 14: Coomassie dye Solution

Reagent	Amount	Final
Methanol	250ml	50%
Coomassie R-250	0,5g	0,1%
MilliQ	200ml	
Acetic Acid	50ml	10%

Table 15: Destain Solution

Reagent	Amount	Final
dH_2O	880ml	
Methanole	50ml	5%
Acetic Acid	70ml	7%

3.4.5. Dialysis

To reduce any toxic shock to the rabbit during the injection of the antigen, it was important to reduce the amount of $NaCl_2$ and sarkosyl. Therefore, fractions containing the SCoAS beta protein were placed in a semipermeable dialysis membrane and submerged in dialysis buffers with decreasing concentrations of sarkosyl and $NaCl_2$. The dialysis membrane was first was placed into a beaker with 500ml of Dialysis buffer A (Table 16) and stirred at 4°C. After one hour, the membrane was transferred into a new beaker with 500ml Dialysis buffer B (Table 17) and again stirred for one hour at 4°C. Finally, it was transferred into the last beaker containing 1 liter of Dialysis buffer C (Table 18) and stirred overnight at 4°C. The following day, the protein was analyzed by Coomassie staining an SDS PAGE gel to verify that the protein remained intact.

Table 16: Dialysis Buffer A

Reagent	Stock	Amount	Final
MilliQ		325ml	
$NaPO_4$	0,1M	100ml	20mM
$NaCl_2$	5M	50ml	500mM
Sarkosyl	20%	25ml	1%

Table 17: Dialysis Buffer B

Reagent	Stock	Amount	Final
MilliQ		362,5ml	
$NaPO_4$	0,1M	100ml	20mM
$NaCl_2$	5M	25ml	250mM
Sarkosyl	20%	12,5ml	0,5%

Table 18: Dialysis Buffer C

Reagent	Stock	Amount	Final
MilliQ		745ml	
$NaPO_4$	0,1M	200ml	20mM
$NaCl_2$	5M	30ml	150mM
Sarkosyl	20%	25ml	0,5%

3.4.6. Protein concentration determination

It is necessary to determine the concentration of the SCoAS beta antigen so we can ensure that we have enough overall protein at a high density for the rabbit injection. The Pierce BCA Protein Assay Kit (Thermo Scientific) was used for the colorimetric detection and quantification of the total protein. A purple-colored product is created by the chelation of BCA molecules with cuprous ions. This results in an absorbance at 562nm that can be measured to determine protein concentrations between 20-2000ug/ml by using a calculation generated from a standard curve made from the serial dilutions of bovine serum albumin (BSA).

First, a set of protein standards was prepared. BSA was diluted with dialysis buffer C to the following concentrations: 2000, 1500, 1000, 750, 500, 250, 125, 25, 0µl/ml. Then, SCoAS beta was diluted with dialysis buffer C to a final volume of 25µl using the following amounts of SCoAS beta: 2,5µl, 5µl, 10µl and 20µl. BSA standards and the diluted SCoAS beta samples were pipetted into a 96 well plate and the BCA working reagent was added. The protein samples were incubated at 37°C for 30 minutes, then cooled to room temperature before the absorbance was measured by the Tecan Infinite M200 plate reader. The absorbance values of the standards were used to create a standard curve and calculating the concentration of the dialyzed SCoAS beta.

3.5. Western blots

A western blot is used to detect a specific protein in a complex sample. In this thesis, we prepared whole cell lysates for western blot analyses from a total of $9x10^7$ to $2x10^8$ cells, depending on the cell density of the culture. WCL were prepared by spinning the cells at 1300g for 10 minutes at 4°C. The supernatant was decanted and the cell pellets were resuspended in 1ml of PBS before being spun down again. An aspirator was used to carefully remove all the supernatant. The cell pellets were then thoroughly resuspended in PBS before adding a 3x SDS PAGE loading dye. These WCL were boiled for 7 minutes

at 97°C to further denature the proteins. The SDS in the loading dye coats the proteins with a negative charge, so they migrate to the positively charged electrode during electrophoresis. Samples prepared in this way were then resolved on a 4-20% gradient polyacrylamide gel (BioRad) by SDS PAGE. The proteins were then transferred onto a PVDF membrane by electroblotting. Prior to transfer, the membrane had to be activated by placing it into methanol for 45 seconds. The blot was then washed in MilliQ water for 2 minutes before soaking with transfer buffer for at least 5 minutes. While equilibrating the membrane, other components for the western blots, including the sponges and whatman papers, were also immersed into the transfer buffer. Finally, a western blot sandwich was made with the following layers: cassette, sponge, paper, gel, paper, sponge and cassette. This sandwich was inserted into the blotting apparatus and the negatively charged proteins were transferred with 90V for 90 minutes.

When the transfer process was done, the blotting sandwich was disabled and the membrane was inserted into a 50ml conical tube. The membrane was then blocked for 1 hour at room temperature in 45ml of 5% milk, which helps to minimize unspecific antibody binding. The membranes were either probed with antibodies on the same day or stored at 4°C overnight. The membranes were probed with specific primary antibodies diluted in 5ml of 5% milk. After rotating for 1 hour at room temperature, they were washed for 15 minutes with 20ml of PBS containing 0.05% Tween 20 (PBS-T). Another three PBS-T washes for 5 minutes were performed to reduce any unspecific binding of the antibody. The blots were then incubated for 1 hour with a secondary antibody conjugated with horseradish peroxidase (HRP) diluted 1:2000 in 5ml of 5% milk. Any excess secondary antibody was again washed in the same way as the primary. Proteins were then visualized with Clarity Western ECL Substrate (BioRad), which produces a chemiluminescent signal on the blot wherever the secondary antibody is bound. The Clarity Western Peroxide Reagent and Clarity Western Luminol/Enhancer Reagent were mixed 1:1 and 500µl was spread over a membrane. After 1 minute, excess ECL was removed from the membrane before it was visualized on the ChemiDoc (BioRad).

4. Results

4.1. SCoAS alpha RNAi growth curve

The depletion of SCoAS beta was previously reported as lethal for BF *T. brucei* cells (Zhang *et al*, 2010), but the same phenotype was not observed by other members of our lab. In order to exhaust all possibilities, we decided to silence the alpha subunit of the SCoAS heterodimeric enzyme in BF *T. brucei* cells. To determine if the loss of this protein produces a growth phenotype, we measured the growth rate of four different SCoAS alpha RNAi clones (HB1, HB3, HB4 and HB6). Cell densities of cultures kept in mid-log phase were counted every 24 hours for 7 days. Cumulative cell densities were then plotted for both noninduced clones and induced cells grown in media with 1ug/ml of tetracycline (Figure 3). No significant growth phenotype was observed for any of the four induced cultures, as the growth curves remained constant between the noninduced and induced cell lines. This would suggest that BF *T. brucei* cultures do not require SCoAS activity when grown in culture, but it must first be verified that these cell lines efficiently targeted the SCoAS alpha mRNA.

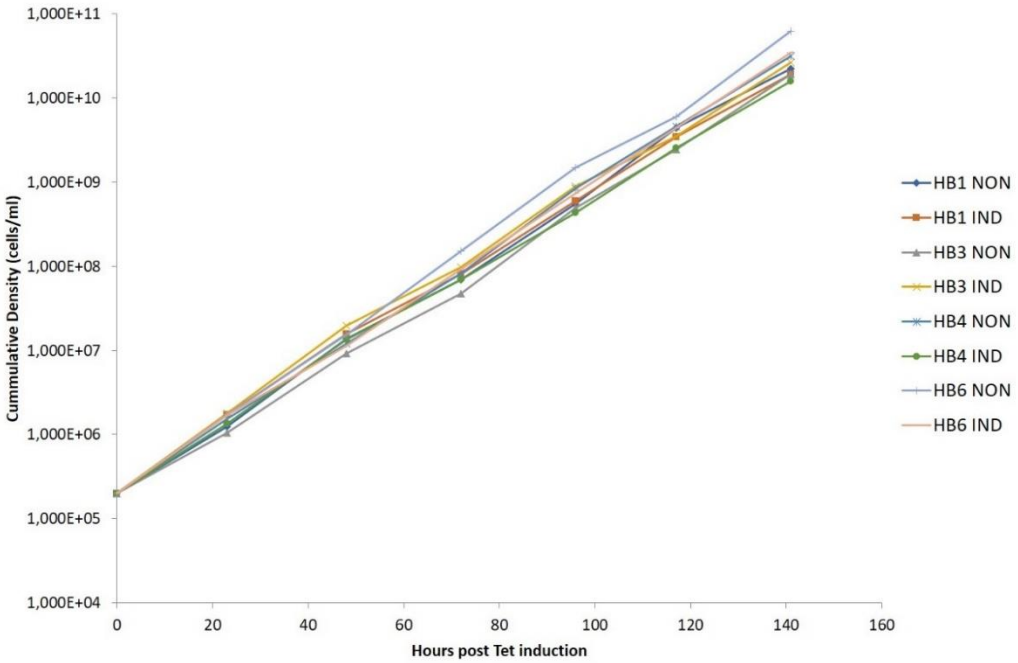

Figure 3: No growth phonotype was observed in multiple BF *T. brucei* SCoAS alpha RNAi cell lines. RNAi was induced by tetracycline for 7 days and the cumulative density of induced cell lines (IND) were compared to noninduced cells (NON).

4.2. qPCR verification of RNAi induction

At the time that the SCoAS alpha RNAi cell lines were generated, we did not have an antibody to recognize this subunit of the enzyme. Therefore, qPCR was performed to verify the efficacy of the SCoAS alpha RNAi to silence the targeted transcript. Total RNA isolated from noninduced parasites and cells induced with tetracycline for 2 and 4 days served as a template to generate cDNA by a reverse transcriptase reaction. This material was then used in a qPCR reaction to calculate the relative amount of the SCoAS alpha transcript detected in induced versus noninduced samples. As a loading control, each SCoAS transcript abundance was normalized to an internal reference gene (18S rRNA or β-tubulin). The calculated results from technical triplicates of clone HB1 were then graphed as the fold change of normalized SCoAS alpha in the induced sample compared to the noninduced sample, with no change in the transcript abundance depicted as 1.0 (Figure 4A). Surprisingly, the cumulative data do not indicate a reduction in the SCoAS alpha transcript. While the levels of the SCoAS alpha transcript remain largely unchanged after two days of RNAi induction, it actually increases drastically on day four when normalized to β-tubulin. Notably, this increase in SCoAS alpha transcript on day four was not observed when the data was analyzed with the 18s internal reference. Since the data were not consistent and generated an unexpected outcome, we took a closer look at the amplification curves generated by the qPCR machine. Then it became obvious that the amplification curves of the internal controls varied between the technical replicates and between the time points. Therefore, we limited the data set to include only the individual replicates that maintained a consistent Ct value for a specific internal reference transcript at each time point. One of the technical replicates had a consistent 18S Ct value at each time point, while another replicate displayed unchanged Ct values for β-tubulin in the uninduced SCoAS RNAi sample and the sample induced for two days of RNAi (Figure 4B). This data set illustrated that the SCoAS alpha transcript was indeed being significantly depleted over time.

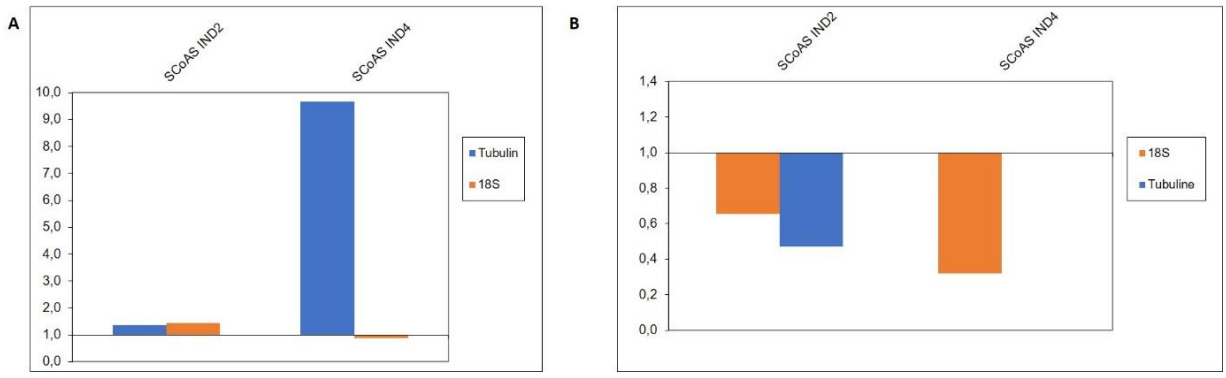

Figure 4: qPCR results of SCoAS alpha RNAi. (A) Cumulative data for three replicates of the HB1 clone were used to calculate the fold change of the SCoAS alpha transcript in RNAi samples induced for two (IND2) or four days (IND4) compared to uninduced samples. Blue columns represent data normalized to the β-tubulin internal reference transcript, while orange columns utilize the 18S transcript as a loading control. (B) The data was analyzed in the same manner, but it only included the replicates with a consistent Ct value of the internal control indicated at each time point.

4.3. SCoAS beta antigen preparation

4.3.1. SCoAS beta protein purification profile

Since the qPCR analysis did not conclusively demonstrate that the RNAi cell line had efficiently depleted the alpha/beta heterodimer SCoAS enzyme, we purified the *T. brucei* SCoAS beta protein to generate a polyclonal antibody that could be utilized in a western blot analysis. It was previously determined that the bacterial expression of SCoAS was largely insoluble. Therefore, after cell lysis with lysozyme, the bacterial pellet was solubilized overnight with 20% sarkosyl. SCoAS beta was then purified on a Ni-NTA column by high performance liquid chromatography (HPLC) using an ÄKTA machine. The protein profile was monitored throughout the purification process by a UV detector (Figure 5). The blue UV trace indicates that a significant amount of solubilized proteins were loaded onto the column before it was washed with buffer A and a new UV baseline was established prior to the protein elution step. As the imidazole concentration was increased linearly, a small but distinct peak is detected in the UV trace, indicating the fractions (29-31) where the majority of the proteins were eluted from the column.

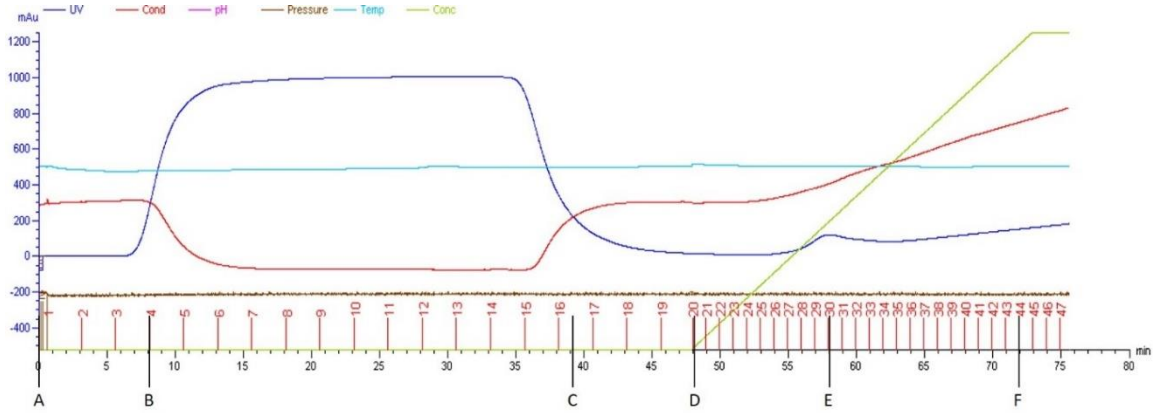

Figure 5: The AKTA UV trace profile of proteins during SCoAS beta purification. A) Equilibration of the column. B) Loading the column with insoluble proteins dissolved in 20% sarkosyl. C) Washing the column. D) Start of the linear imidazole gradient to elute proteins bound to the column. E) Peak fractions with the eluted protein. F) Completion of the imidazole gradient. The type of detectors used for each of the color coded traces are indicated at the top of the image. Importantly, UV detected proteins are shown in blue, while the imidazole concentration is a light green.

4.3.2. SDS PAGE

To verify that the peak elution fractions detected by the UV detector contained a protein of the expected size, samples from throughout the purification process were resolved on a polyacrylamide gel and stained with Coomassie blue G250 (Figure 6). The expected size of the recombinant SCoAS beta protein is 44 kDa and unexpectedly, we don't detect a significant band of this size in the bacterial whole cell lysate. However, a protein migrating at the expected size is observed in the fractionated samples, with the majority of the protein observed in the insoluble fraction, as previously reported. Importantly, this same band is barely detected in the flow through fractions, indicating that almost all of the His-tagged SCoAS beta was bound to the nickel column. Finally, almost all of the 44 kDa protein is visible in fractions 28-32, which corresponds to the UV peak. These fractions are also very clean, as there are very few other detected proteins contaminating the sample.

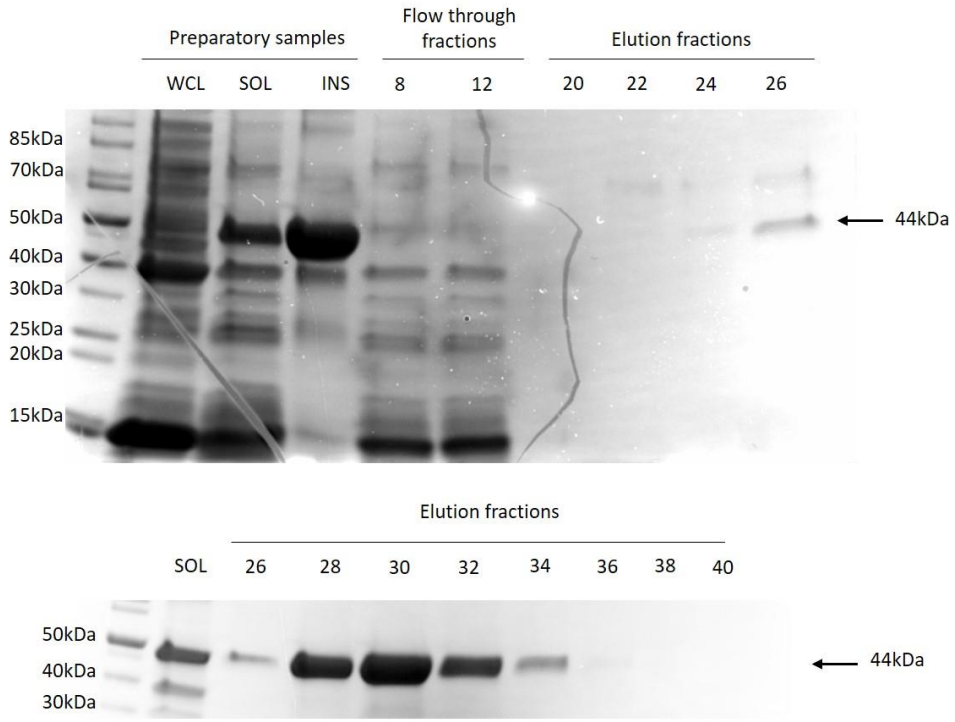

Figure 6: Analysis of AKTA SCoAS affinity purification by Coomassie staining. Proteins resolved on a polyacrylamide gel were fixed and then strained with Coomassie G250. 30µl of all samples were loaded. WCL – bacterial whole cell lysate, SOL – soluble fractions, INS – insoluble fractions. The fraction numbers correlate with the numbers depicted in the purification profile in Figure 5.

While the sarkosyl was effective in solubilizing the recombinant SCoAS beta, the concentration needed to be reduced to limit the toxicity of the antigen injected into the rabbit. Therefore, fractions 28-32 were pooled and then dialyzed to remove the excess sarkosyl and reduce the high salt content required during the purification to reduce unspecific proteins binding to the column. Before shipping the protein to David's Biotechnology for antibody preparation, the quality of the purified SCoAS beta protein was verified once more. The Coomassie stained polyacrylamide gel (Figure 7.) revealed there was just a single band of the expected size, indicating that the protein was not degraded or negatively influenced by the dialysis and storage conditions. Final concentration of 550µg/ml of soluble recombinant protein was shipped.

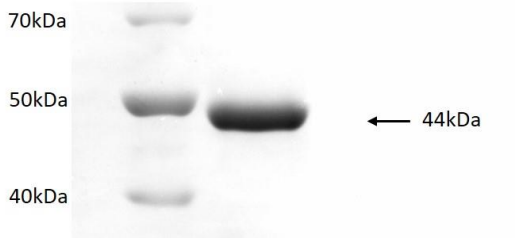

Figure 7: Purity and integrity of purified SCoAS beta submitted to David's Biotechnology for polyclonal antibody production. Fractions 28 through 32 (Fig 4) were pooled and dialyzed. 30 µl of the resulting protein sample was resolved on polyacrylamide gel and stained with Coomassie.

4.4.Testing SCoAS beta PAb

Once we received the polyclonal rabbit SCoAS beta antibody from David's Biotechnology, we determined the specificity and avidity of the antibody. The rabbit producing the antibody had a significant final titer of 1:300,000. The polyclonal antibody was also affinity purified with our soluble SCoAS beta antigen bound to a column. Therefore, we tested the SCoAS beta PAb on $1x10^7$ whole cell lysates prepared from PF, BF and dyskinetoplastic (Dk) trypanosomes (Figure 8). Since we anticipated a strong antibody, a western blot was probed with the rabbit anti-SCoAS beta antibody diluted 1:1000 in 5% milk. The secondary HRP goat anti-rabbit antibody was diluted 1:2000 in 5% milk. Proteins were then visualized by ECL on the ChemiDoc (BioRad). A single band at the expected size of 44 kDa was detected in the protein-rich whole cell lysate samples, suggesting that the antibody has high specificity for SCoAS beta. As expected, the highest levels of SCoAS expression were observed in the PF cells, which correlates with the substrate-level phosphorylation activity detected in PF mitochondria (Bochud-Allemann, 2002). While the BF sample has lower amounts of SCoAS beta, its detection corroborates the mass spectrometry data from the BF mitochondrion (Zíková *et al*, 2017). Comparatively, the Dk trypanosomes that lack mitochondrial DNA had significantly lower expression levels of SCoAS beta.

Figure 8: Western blot analysis of SCoAS beta expression in PF, BF & Dk *T. brucei*. Whole cell lysates (WCL) were prepared from PF, BF and Dk. $1x10^7$ WCL were resolved on a polyacrylamide gel. Proteins were then transferred to a PVDF membrane, which was probed with the anti-SCoAS beta antibody diluted 1:1000 in 5% milk.

Since western blot analyses are usually performed on a single cell type, we analyzed how much material needs to be loaded to effectively detect SCoAS beta from PF, BF and Dk whole cell lysates (Figure 9). Importantly, each blot of a specific cell type was exposed individually. The intense PF bands were easily detected, with a short exposure time. $3x10^6$ WCL was more than enough to create a strong signal and it would probably be possible to dilute the antibody 1:2000 even with this smaller number of WCL. Although the exposure time was longer, the BF and Dk cell lines also had an intensive band already at $3x10^6$ WCL. Therefore, $3x10^6$ WCL is enough for detecting SCoAS beta with the antibody diluted at least 1:1000.

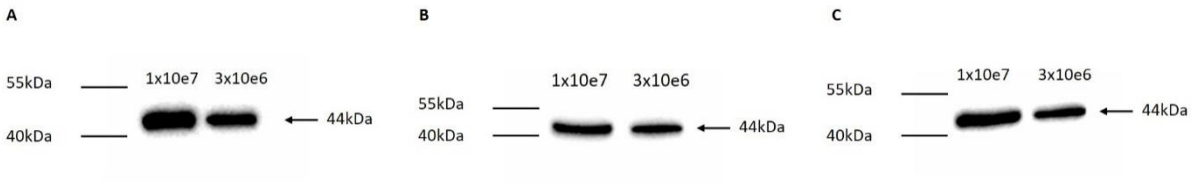

Figure 9: Amount of whole cell lysates needed to detect SCoAS expression in PF, BF and Dk trypanosomes. Two different amounts of WCL were resolved on a polyacrylamide gel, transferred to a membrane and probed with the anti-SCoAS beta antibody diluted 1:1000 in 5% milk. The exposure times were optimized for each cell line A) PF WCL, B) BF WCL, C) Dk WCL.

Generating a PAb is expensive and the antibody itself is a very valuable tool, therefore it is important to determine the best long-term storage conditions to maximize the lifespan of the PAb. Therefore, 3 aliquots of the SCoAS beta PAb were made and stored under different conditions. The control remained at 4°C, while the other two aliquots were stored at -20°C. Since freezing a sample will create ice crystals that could damage the antibody, we diluted one of the -20°C aliquots 1:1 with 100% glycerol. After one week, the best long-term storage conditions were analyzed (Figure 10). Storage in -20°C slightly decrease the efficiency of the antibody. Adding 100% glycerol did not appear to help protect the antibody, it possibly even decreased the efficiency a little bit more. Since antibody storage at 4°C is only recommended for short periods of time (weeks to a few months), we decided to create small 50ul aliquots without glycerol that were stored in a dedicated -20°C without the frost freeze option. Once thawed, the working aliquot will remain at 4°C to avoid multiple freeze/thaw cycles.

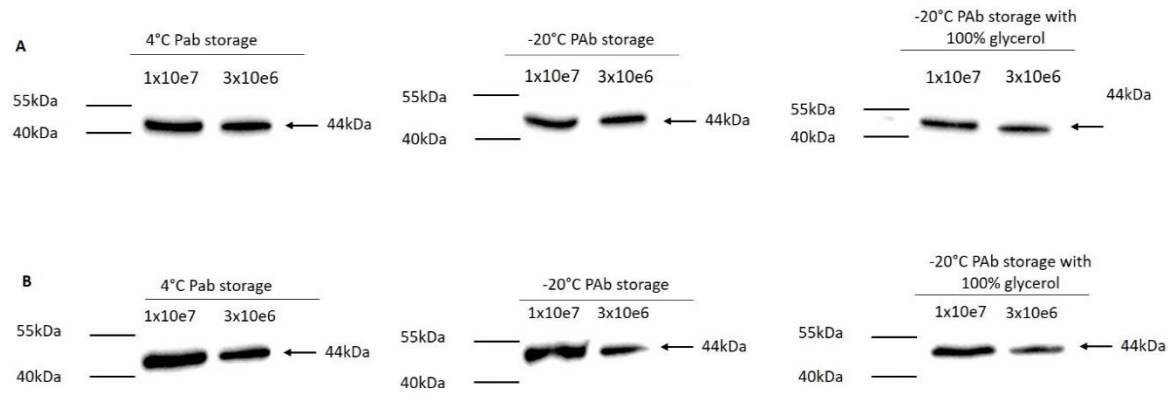

Figure 10: Analyzing the best long-term storage conditions for the SCoAS polyclonal antibody. Two different WCL amounts of A) BF and B) Dk were probed with different antibody aliquots that were stored for one week under the conditions described. The SCoAS beta antibody was diluted 1:1000 in 5% milk.

4.5. Verification of SCoAS cell lines

4.5.1. SCoAS beta RNAi

While western blots with the SCoAS beta antibody detected a single band of the expected size, it is important to genetically verify that the antibody recognizes SCoAS beta. Therefore, we prepared whole cell lysates from the SCoAS beta RNAi cell line that was either noninduced or induced for 1, 2 or 3 days with tetracycline. A western blot containing $1x10^7$ WCL samples from two SCoAS beta RNAi clones were probed with the SCoAS beta antibody diluted 1:1000 in 5% milk (Figure 11). A significant decrease of SCoAS beta was already visible after the first day of RNAi induction and this decrease progressed each day until the signal was almost undetectable by day 3. To determine the RNAi efficiency to deplete SCoAS beta, an antibody that recognizes adenine phosphoribosyltransferase (APRT) was used as a loading control. APRT is a purine salvage enzyme localized to the cytosol that was previously characterized in BF *T. brucei* cells. The signal intensity of SCoAS beta bands in each sample was normalized to the amount of APRT in the same sample. The percentage of SCoAS expression for each sample was then calculated by comparing the normalized values of the RNAi induced samples to the uninduced samples. Since there was less than 5% SCoAS expression remaining in the day 3 RNAi induced cell lines, it is accurate to conclude that the BF *T. brucei* cultures do not require SCoAS activity.

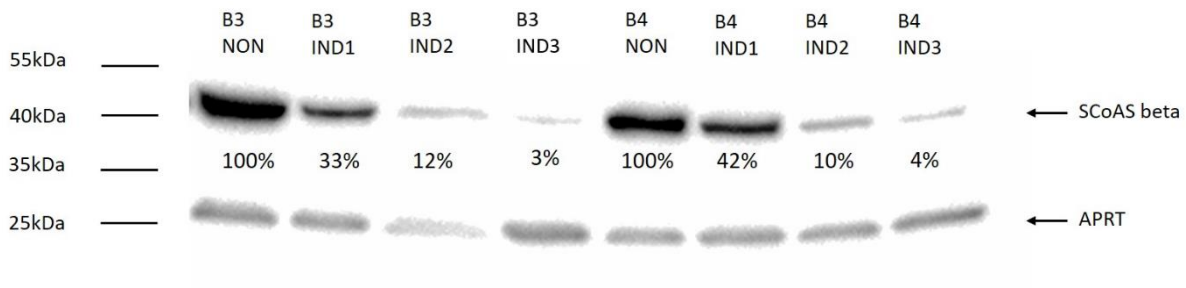

Figure 11: Verifying the specificity of the SCoAS polyclonal antibody. WCL from SCoAS beta RNAi cells were made from clones B3 and B4 before (NON) and after induction (IND 1-3). WCL from $1x10^7$ cells were resolved on a polyacrylamide gel. SCoAS beta antibody was diluted 1:1000. APRT expression levels were used as a loading control to calculate the amount of SCoAS beta detected in each sample as compared to the uninduced sample.

4.5.2. SCoAS alpha RNAi

For further verification that the SCoAS enzyme exists as heterodimer, we examined the expression levels of SCoAS beta in the SCoAS alpha RNAi cell line. Similar as above, whole cell lysates were prepared from uninduced SCoAS alpha RNAi and cultures induced with tetracycline for 3 days. A western blot containing WCL of $1x10^7$ cells from clones HB4 and HB6 were analyzed with the SCoAS beta antibody diluted 1:1000. Once again, APRT was used as loading control and the proteins were visualized on the ChemiDoc (Figure 12). The results demonstrate that SCoAS beta is progressively depleted over time, suggesting that the stability of SCoAS beta depends on the expression of SCoAS alpha.

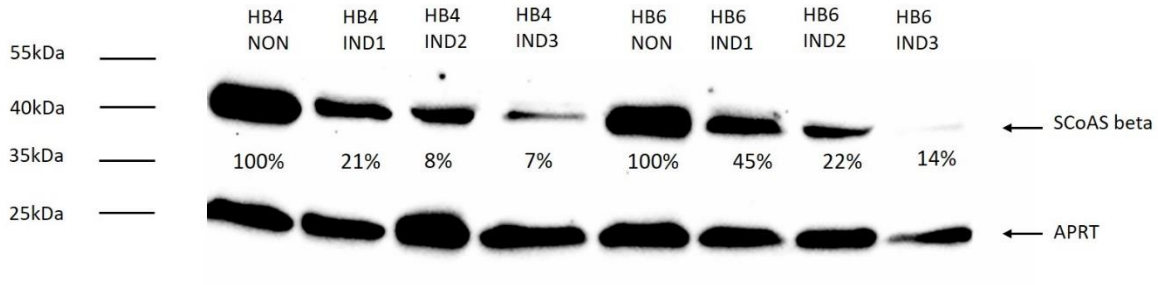

Figure 12: Verification of an SCoAS heterodimer as the depletion of SCoAS alpha destabilizes beta. WCL from SCoAS alpha RNAi cells were made from clones HB4 and HB6 before (NON) and after induction (IND 1-3). WCL from $1x10^7$ cells were resolved on a polyacrylamide gel. The SCoAS beta antibody was diluted 1:1000 dilution. APRT expression levels were used as a loading control.

4.5.3. MiTaT SCoAS beta RNAi

Since it was previously reported that SCoAS beta was essential for BF *T.brucei*, we wanted to examine the SCoAS beta RNAi depletion in another *T. brucei* lab strain. Therefore, we utilized the BF *T. brucei* Lister 427 MiTat 90-13 cell line that we received as a generous gift from the Bringaud lab. The MiTat SCoAS beta RNAi cells were previously generated by another lab member. As above, the whole cell lysates from $1x10^7$ cells were prepared from uninduced and induced cultures. This time, the mitochondrial heat shock protein 70 (mtHsp70) was used as loading control. mtHsp70 is an essential mitochondrial chaperone with various functions. It is involved in mitochondrial protein import, assists in the folding of proteins and participates in mitochondrial DNA maintenance. As for the previous cell line, there is a significant decrease of SCoAS beta levels when normalized to mtHSP70 (Figure 13). In fact, the protein was completely undetected by the third day of RNAi induction.

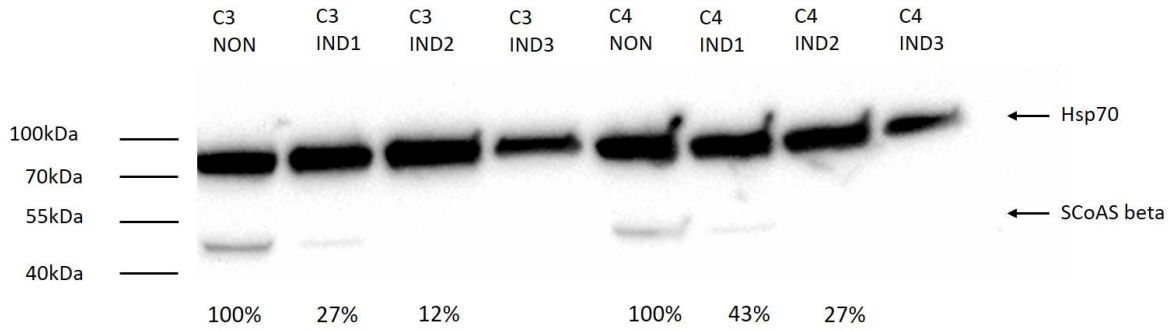

Figure 13: Verification of the SCoAS beta RNAi efficiency in the *T. brucei* MiTat cell line. WCL from SCoAS beta RNAi cells were made from clones HB4 and HB6 before (NON) and after induction (IND 1-3). WCL from $1x10^7$ cells were resolved on polyacrylamide gel. SCoAS beta antibody was used in 1:1000 dilution. mtHSP70 expression levels were used as a loading control.

5. Discussion

The results presented in this thesis show no visible growth phenotype caused by SCoAS depletion by RNAi. This is in contrast with the data presented by Zhang *et al.* They suggest that SCoAS beta depletion is lethal not only for PF T. *brucei*, but also for BF parasites. A rapid growth phenotype was observed already after 20 hours of RNAi induction. Such a fast lethal effect seems unusual, since the silencing of essential protein expression by RNAi is not typically observed until 48 or 72 hours of induction. Zhang verified their results by a northern blot analysis of the RNA isolated from various SCoAS beta RNAi time points. While there was no detectable signal after 18 hours of induction, the visualized amount of total RNA loaded might suggest that less of the induced sample was used, which could influence the final results. The elimination of the target RNA at such an early time point suggests an incredibly efficient RNAi system, that if coupled with a protein that has a very short half-life, could result in such an extreme growth phenotype.

RNAi as a gene silencing mechanism is not completely reliable without some further verifications. There is some tolerance for mismatches and gaps in base pairing with targets (Ma *et al, 2006*), which can influence different mRNAs, not just the targeted one. Also, some genes can have a portion of their sequence with partial complementarity to another region of the genome, which can cause multiple RNA molecules to be ablated (Rual *et al,2007*). This off-target effect can lead to false positive results. In fact, depending on the specificity of the chosen RNAi sequence, it can be responsible for even 30% of all positive results (Fedorov *et al, 2006*). These possibilities vary from 5 to 80% between organisms (Qiu *et al, 2005*). The risk of off-target effects can be influenced or predicted. For example, the untranslated regions of a transcript are much more likely to contain repetitive sequences throughout the genome than the coding region of a gene. Therefore, limiting the targeted RNA to a coding sequence can curb the possibility of RNAi off-target effects. In addition, the length of the RNAi molecule can determine the probability of unintended consequences. The ideal length of siRNA in mammalian cells is 21 nucleotides, with increasing dsRNA sizes allowing for more possible mismatches (Qiu *et al, 2005).* However, it has already been determined that the generation of dsRNAi between 400-600 nucleotides produces the most efficient RNAi in *T. brucei*.

Unfortunately, the Zhang *et al.* paper does not include any information about the SCoAS beta dsRNAi sequence chosen or the type of RNAi vector they used in their experiments. Therefore, it is not possible to duplicate their RNAi cell line with exactly the

same RNAi approach. Furthermore, Zhang *et al.* did not address the issue of a possible off-target effect. To eliminate this possibility, the expression of an RNAi resistant ectopic copy of the targeted gene should alleviate the growth phenotype. This heterologous gene would need to be encoded with an alternative nucleotide at the wobble position of every codon, while still retaining the same primary amino acid sequence. If desired, this heterologous gene expression can be regulated by utilizing the constitutive expression of the T7 RNA polymerase and the bacterial Tet repressor already present in the RNAi cell line. The *T. brucei* genome integrated vector epressing the RNAi resistant SCoAS beta coding sequence will be preceded by the T7 promotor and the Tet repressor DNA sequence. Therefore, tetracycline added to the cell culture will bind the Tet repressor, causing a conformational change that will remove the protein from the DNA sequence. If the dsRNAi silences only the intended gene product, then the addition of tetracycline should reduce the intensity of the SCoAS beta growth phenotype observed in the Zhang *et al.* paper. Unfortunately, the Ochsenreiter lab was not able to locate the original SCoAS beta RNAi cell line for us to implement this control.

Another important distinction and possible reason for the different SCoAS beta RNAi results revolves around the *T. brucei* lab strains utilized. The parasites can be grown for some limited time (1-2 months) in axenic culture before they start to accumulate modifications that can limit the effectiveness of regulatable RNAi or restrict the flexibility of various biological processes. If the cells are kept too long in culture, they can become altered to the extent that two previously identical clones can produce different phenotypes from the same genetic modification. Therefore, it is critical to limit the time of any cell line kept in culture by making stabilates that can be stored long-term in liquid nitrogen. A classic example of the parasite irreversibly adapting to the artificial conditions of an *in vitro* culture is best illustrated when the parasite loses the ability to differentiate and complete a full life cycle. BF *T. brucei* parasites are pleomorphic in a mammalian host. This means that their cell morphology changes as they undergo a developmental transition from the proliferative long slender form to the quiescent short stumpy forms, which are pre-adapted to survive in the tsetse fly (Mony *et al*, 2015). In order to retain this pleomorphic ability, the cultured parasites must be routinely passed through an animal. In comparison, when pleomorphic cell lines are kept in culture for extended periods of time (months), they become monomorphic strains that are similar to the naturally occurring slender form. However, these parasites are not able to differentiate into the stumpy form.

Instead, they must be coaxed with high concentrations of citrate/cis-aconitase to partially differentiate into the procyclic form *in vitro* (Rico *et al*, 2013).

Another significant factor to be reconciled when attempting to recreate the same result from another lab is the media used to cultivate the cells *in vitro*. The standard media used throughout the *T. brucei* community is the semi-defined HMI-11. The variability in the media arises from the addition of 10% FBS, where the concentration of each component might vary between lots. HMI-11 has multiple energy sources, amino acids and vitamins, most of which are in abundance. To address this issue, metabolomics data was used to create CMM media, which more closely resembles the nutrients found in the blood of the mammalian host, e.g., reduced concentrations of glucose and amino acids like cysteine or glutamine (Creek *et al*, 2013). While BF *T. brucei* can uptake multiple carbon sources, it prefers glucose to all others. When provided high levels of glucose, glycolysis becomes the central metabolic pathway that can define all the other bioenergetics of the cell. Therefore, adapting the cultured parasites to CMM can take weeks, even though the media is simply reducing the excess availability of a few metabolites. Interestingly, a colleague in the lab has observed a slight growth phenotype in SCoAS beta RNAi induced cells grown in CMM media, demonstrating that the nutritional value of the media can influence the metabolism of the parasite.

Furthermore, while CMM simulates the nutritional environment of mammalian blood better than HMI-11, it is not commonly used in the field. Furthermore, neither of these media can simulate the host immune system. The plasma membrane of BF *T. brucei* has a densely packed layer of an identical surface glycoprotein that can be internalized and replaced with a variant when it is recognized by a host antibody (Fenn *et al*, 2007). Since this process is very energy demanding, this could create differences in the ATP requirements between cultivated cells and parasites residing in the mammalian bloodstream. Indeed, another student in the lab has found that the virulence of *T. brucei* parasites lacking SCoAS is significantly decreased in a mouse model.

It has also been previously demonstrated that different phenotypes can be observed when different lab strains of BF *T. brucei* are used. For example, a study on the F_OF_1-ATP synthase in PF *T. brucei* Lister 427 cells demonstrated that the depletion of subunit α resulted in a significant growth phenotype (Zíková *et al* 2009). Meanwhile, the same RNAi experiment performed in another lab using PF T. brucei EATRO 1125 produced

only a very mild growth phenotype (Coustou *et al* 2008). Because of these differences, RNAi of SCoAS beta was tested not only in our BF *T. brucei* Lister 427 lab strain, but also in the *T. brucei* Lister 427 MiTat 1.2. cells used in Zhang paper. However, SCoAS beta RNAi in the MiTat 1.2 strain did not result in any growth phenotype and the levels of SCoAS beta depletion are very similar to the ones in the Lister 427 strain from our lab.

While RNAi is a powerful and quick method to assess the function of a gene product, it usually does not result in the complete elimination of the targeted mRNA and some of the protein will still remain. The amount of the active enzyme remaining could play a crucial role, since even a small amount could be sufficient for cell survival. However, the results presented in this thesis indicate that the RNAi is very efficient and the remaining amount of either SCoAS beta or alpha would not seem sufficient for ATP production in the BF mitochondrion. Still, to eliminate any doubts, it is necessary to generate an SCoAS beta double knockout cell line, in which both alleles have been replaced by selectable markers. This process was completed by another lab member, who is currently characterizing how the loss of SCoAS effects the energy metabolism of the parasite.

6. References

Berriman, M., Ghedin, E., & Hertz-Fowler, C. (2005). The Genome of the African Trypanosome Trypanosoma brucei. *Science,309*(5733), 416-422.

Bochud-Allemann, N., & Schneider, A. (2002). Mitochondrial Substrate Level Phosphorylation Is Essential for Growth of Procyclic Trypanosoma brucei. *Journal of Biological Chemistry*, 277(36), 32849-32854.

Bringaud, F., Rivière, L., & Coustou, V. (2006). Energy metabolism of trypanosomatids: Adaptation to available carbon sources. *Molecular and Biochemical Parasitology,149*(1), 1-9.

Burri, Ch., & Chappuis, F. (2014). Human African Trypanosomiasis. *Mansons Tropical Infectious Diseases*.

Coustou, V., Biran, M., Breton, M., Guegan, F., Rivière, L., and et al. (2008). Glucose-induced Remodeling of Intermediary and Energy Metabolism in Procyclic Trypanosoma brucei. *Journal of Biological Chemistry,283*(24), 16342-16354.

Creek, D. J., Nijagal, B., Kim, D., Rojas, F., Matthews, K. R., & Barrett, M. P. (2013). Metabolomics Guides Rational Development of a Simplified Cell Culture Medium for Drug Screening against Trypanosoma brucei. *Antimicrobial Agents and Chemotherapy,57*(6), 2768-2779.

Croft, S., Barrett, M., & Urbina, J. (2005). Chemotherapy of trypanosomiases and leishmaniasis. *Trends in Parasitology,21*(11), 508-512.

Cross, G. A., & Manning, J. C. (1973). Cultivation of Trypanosoma brucei sspp. in semi-defined and defined media. *Parasitology*, 67(03), 315.

Eadsforth, T. C., Cameron, S., & Hunter, W. N. (2012). The crystal structure of Leishmania major N5,N10-methylenetetrahydrofolate dehydrogenase/cyclohydrolase and assessment of a potential drug target. *Molecular and Biochemical Parasitology*, 181(2), 178-185.

Fedorov, Y., & Anderson, E. M. (2006). Off-target effects by siRNA can induce toxic phenotype. *Rna,12*(7), 1188-1196.

Fenn, K., & Matthews, K. R. (2007). The cell biology of Trypanosoma brucei differentiation. *Current Opinion in Microbiology,10*(6), 539-546.

Hunger-Glaser, I., Linder, M., & Seebeck, T. (1999). Histidine-phosphorylation of succinyl CoA synthetase from Trypanosoma brucei. *Molecular and Biochemical Parasitology,100*(1), 43-52.

Hunt, M., & Köhler, P. (1995). Purification and characterization of phosphoenolpyruvate carboxykinase from Trypanosoma brucei. *Biochimica Et Biophysica Acta (BBA) - Protein Structure and Molecular Enzymology,1249*(1), 15-22.

Jenkins, T. M., Eisenthal, R., & Weitzman, P. J. (1988). Two distinct succinate thiokinases in both bloodstream and procyclic forms of Trypanosoma brucei. *Biochemical and Biophysical Research Communications,151*(1), 257-261.

Johnson, J. D., Mehus, J. G., Tews, K., Milavetz, B. I., & Lambeth, D. O. (1998). Genetic Evidence for the Expression of ATP- and GTP-specific Succinyl-CoA Synthetases in Multicellular Eucaryotes. *Journal of Biological Chemistry*, 273(42), 27580-27586.

Ma, Y., Creanga, A., Lum, L., & Beachy, P. A. (2006). Prevalence of off-target effects in Drosophila RNA interference screens. *Nature,443*(7109), 359-363.

Millerioux, Y., Morand, P., Biran, M., Mazet, M., Moreau, P., and et al (2012). ATP Synthesis-coupled and -uncoupled Acetate Production from Acetyl-CoA by Mitochondrial Acetate:Succinate CoA-transferase and Acetyl-CoA Thioesterase in Trypanosoma. *Journal of Biological Chemistry*, 287(21), 17186-17197.

Mony, B. M., & Matthews, K. R. (2015). Assembling the components of the quorum sensing pathway in African trypanosomes. *Molecular Microbiology,96*(2), 220-232.

Pfaffl, M. W. (2001). A new mathematical model for relative quantification in real-time RT-PCR. *Nucleic Acids Research*, 29(9).

Poon, S. K., Peacock, L., Gibson, W., Gull, K., & Kelly, S. (2012). A modular and optimized single marker system for generating Trypanosoma brucei cell lines expressing T7 RNA polymerase and the tetracycline repressor. *Open Biology*, 2(2).

Qiu, S., & Adema, C. M. (2005). A computational study of off-target effects of RNA interference. *Nucleic Acids Research,33*(6), 1834-1847.

Rico, E., Rojas, F., Mony, B. M., Szoor, B., Macgregor, P., & Matthews, K. R. (2013). Bloodstream form pre-adaptation to the tsetse fly in Trypanosoma brucei. *Frontiers in Cellular and Infection Microbiology,3*.

Rual, J., Klitgord, N., & Achaz, G. (2007). Novel insights into RNAi off-target effects using C. elegans paralogs. *BMC Genomics,8*(1), 106.

Schnaufer, A., Clark-Walker, G. D., Steinberg, A. G., & Stuart, K. (2005). The F1-ATP synthase complex in bloodstream stage trypanosomes has an unusual and essential function. *The EMBO Journal,24*(23), 4029-4040.

Smith, Terry K., & Bringaud, F., (2017). Metabolic Reprogramming during the Trypanosoma Brucei Life Cycle. *F1000Research*, vol. 6, p. 683.

Sommer, J. M., Nguyen, T. T., & Wang, C. (1994). Phosphoenolpyruvate carboxykinase of Trypanosoma brucei is targeted to the glycosomes by a C-terminal sequence. *FEBS Letters,350*(1), 125-129.

Taleva, G. (2016). Bioenergetics of the *Trypanosoma brucei* bloodstream form. Literature Review

Van Hellemond, J., Opperdoes, F. R., & Tielens, A. G. (2005). The extraordinary mitochondrion and unusual citric acid cycle in Trypanosoma brucei. *Biochemical Society Transactions,33*(5), 967-971.

Van Hellemond, J., Opperdoes, F. R., & Tielens, A. G. (1998). Trypanosomatidae produce acetate via a mitochondrial acetate:succinate CoA transferase. *Proceedings of the National Academy of Sciences,95*(6), 3036-3041.

Vickers, T. J., Murta, S. M., Mandell, M. A., & Beverley, S. M. (2009). The enzymes of the 10-formyl-tetrahydrofolate synthetic pathway are found exclusively in the cytosol of the trypanosomatid parasite Leishmania major. *Molecular and Biochemical Parasitology,166*(2), 142-152.

Wirtz, E., Leal, S., Ochatt, C., & Cross, G. (1999). A tightly regulated inducible expression system for conditional gene knock-outs and dominant-negative genetics in Trypanosoma brucei. *Molecular and Biochemical Parasitology*, 99(1), 89-101.

Zhang, X., Cui, J., Nilsson, D., Gunasekera, K., Chanfon, A., and et al (2010). The Trypanosoma brucei MitoCarta and its regulation and splicing pattern during development. *Nucleic Acids Research,38*(21), 7378-7387.

Zíková, A., Schnaufer, A., Dalley, R. A., Panigrahi, A. K., & Stuart, K. D. (2009). The F0F1-ATP Synthase Complex Contains Novel Subunits and Is Essential for Procyclic Trypanosoma brucei. *PLoS Pathogens,5*(5).

Zíková, A., Verner, Z., Nenarokova, A., Michels, P. A., & Lukeš, J. (2017). A paradigm shift: The mitoproteomes of procyclic and bloodstream Trypanosoma brucei are comparably complex. *PLOS Pathogens,13*(12).